energies

Article

A Design of a 2 DoF Planar Parallel Manipulator with an Electro-Pneumatic Servo-Drive—Part 2

Jakub Takosoglu *, Urszula Janus-Galkiewicz and Jaroslaw Galkiewicz

Faculty of Mechatronics and Mechanical Engineering, Kielce University of Technology, Aleja Tysiaclecia Panstwa Polskiego 7, 25-314 Kielce, Poland
* Correspondence: qba@tu.kielce.pl

Abstract: This paper is the second part of the study of a planar manipulator and this section presents the construction of a prototype manipulator. A fuzzy control system for the manipulator is described in detail. An experimental study was carried out on the positioning of the end effector of the manipulator and a program written in the Delphi 6 environment was proposed to calculate the position. Prototype tests were performed for transpose and follow-up control. Based on the experimental results, a control quality analysis was carried out.

Keywords: planar parallel manipulator; fuzzy logic controller; pneumatic positioning system; electro-pneumatic servo-drive

check for updates

Citation: Takosoglu, J.; Janus-Galkiewicz, U.; Galkiewicz, J. A Design of a 2 DoF Planar Parallel Manipulator with an Electro-Pneumatic Servo-Drive—Part 2. *Energies* **2023**, *16*, 2970. https://doi.org/10.3390/en16072970

Academic Editor: Anibal De Almeida

Received: 11 December 2022
Revised: 10 March 2023
Accepted: 12 March 2023
Published: 24 March 2023

1. Introduction

Pneumatic drive and control play an important role in various industries. Manufacturing companies are increasingly automating production processes using robots and manipulators, with pneumatic manipulators being a common solution due to their low operating costs. Pneumatic issues are also a popular topic among researchers, as evidenced by numerous articles.

The solution to the simple kinematics problem of most known plane structures of parallel manipulators was presented by Merlet [1]. The manipulator structures analyzed were built from three identical kinematic chains. Merlet has shown that from the direct kinematics viewpoint, all the possible kinematic chains can be reduced to a member of a set of three basic chains. Merlet et al., in the paper [2], presented geometrical algorithms for the determination of the boundary of various workspaces for planar parallel manipulators. Performance evaluation of two-degrees-of-freedom planar parallel robots was presented by Feng Gao et al. [3]. To get establish analytical relationships between the links' lengths of the two-degrees-of-freedom parallel planar robots and the indicators of control quality based on the global conditioning and velocity indices, a geometric model of the solution space was applied. The model was also utilized to develop charts useful for the analysis and design of the mechanisms.

The 3-PRR parallel manipulator, kinematics analysis, and a description of the boundaries of the workspace can also be found in the literature [4,5]. The authors state that the manipulators can find applications in motion simulators or other high-precision or high-speed devices.

Feng Gao et al. [6] studied the problem of the relationship between the workspace shapes and the dimensions of the links of 3-DOF symmetrical planar parallel robots. The designers can easily use the results to optimize the structure of the robots. Heerah et al. [7] compared several planar fully parallel robots with three identical kinematic chains. The authors concluded that a 3-PRR configuration is the most appropriate for the electronic parts assembly industry.

In the work [8], the most popular parallel robots were analyzed, taking into account the number of degrees of freedom or the type of joints connecting the manipulator elements.

The most common structures of parallel robots with closed kinematic chains were considered, for which the shapes of the working spaces were determined, taking into account geometrical constraints. The work contains several examples of parallel robots.

The development of the drive systems of traditional machine tools with a Cartesian axis system increases the accuracy required and increases the rigidity of the machine tool, thus increasing its weight and size., which were required to achieve high mobility and high dynamics. This, in turn, resulted in the creation of slender kinematic structures in the form of devices with a parallel kinematic chain, allowing for high dynamics while maintaining the high rigidity of the robot. The masses moved can be much larger than those moved by traditional linear robots. In devices currently manufactured, the differences between an industrial robot and a machine tool are blurred, especially in hybrid structures. Parallel kinematic robots resemble truss elements in appearance, in which masses and loads are distributed over bars. The constructions resulting from the combination of serial and parallel manipulators, called hybrid robots, are developing most dynamically. They allow you to combine the advantages of both types of machines.

At present, plane constructions of robots with closed kinematic chains are very popular. They are used in fast production processes, e.g., sorting of details, palletizing, sorting, waste segregation, and laser marking, among others. Depending on the application, robots can be driven not only by pneumatic drives but by other methods. In many applications, piezoelectric drives could be more appropriate due to their dynamic properties [9].

Apart from creating new robots, detailed analyses are provided to improve the functional properties of parallel robots. To increase the effectiveness of the application parallel, robots can be optimized by the application of procedures that minimize trajectory time and increase the workspace [10]. On the other hand, a detailed study of robots can increase the precision of the effector movement by taking into account geometric errors [11].

In one article, [12] the theoretical basis for the manipulator with a pneumatic drive controlled by a fuzzy-logic controller had been provided. In the present article, the prototype of the manipulator is tested.

2. The Design and Construction of a Prototype Manipulator

Based on the simulation and design studies presented in the previous paper [12], a prototype planar parallel pneumatic manipulator with two degrees of freedom was constructed. The 3D model was the reference for making the prototype manipulator (Figure 1).

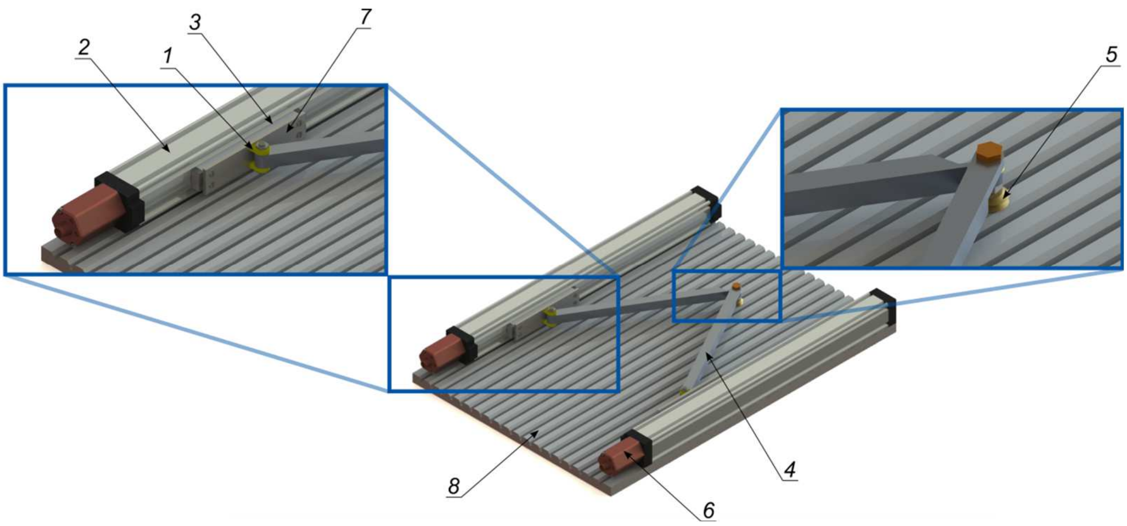

Figure 1. A solid model of a parallel manipulator: 1—bearing, 2—actuators, 3—actuator sliders, 4—arms, 5—end effector, 6—position transducers, 7—mounting plates, 8—baseplate.

A general view of the prototype manipulator is shown in Figure 2.

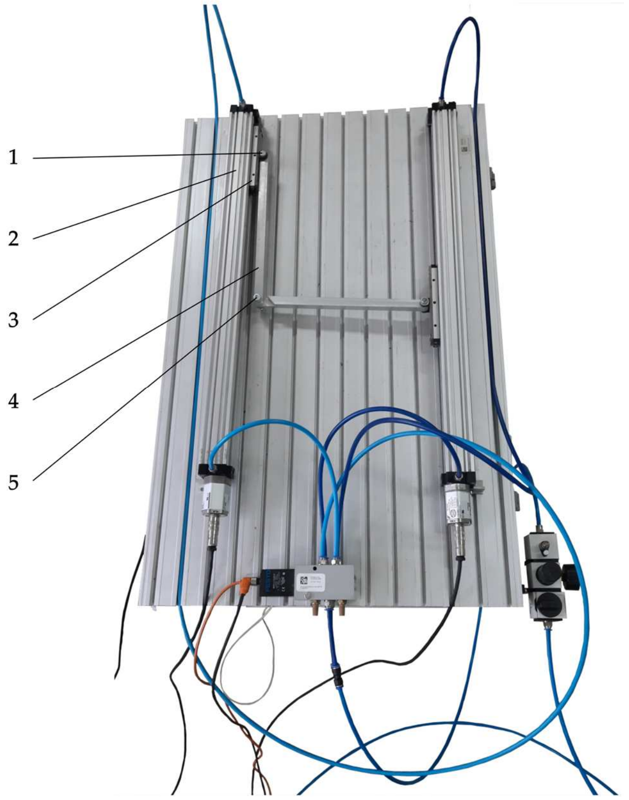

Figure 2. A general view of the prototype plane parallel pneumatic manipulator: 1—joint, 2—rodless actuator, 3—actuator slide, 4—manipulator arm, 5—end effector.

The following components were used to build the manipulator:

- 11.500D.00120ZS rodless actuators by CPP PREMA,
- ESTM-08-SL stand bearings by IGUS,
- plain bearings JFM-1012-05F by IGUS,
- 5/3 MPYE-5-1/8-HF servo-valves by FESTO,
- FR-C4i compressed air preparation unit by Bosch-Rexroth,
- Aluminium arms (18 mm × 18 mm).

3. Control System

The servo-pneumatic axes of the manipulator are equipped with a magnetostrictive position and speed transducers with an analog output. The actuators are controlled by two 5/3 (five-way three-position) servo-valves. Rapid control prototyping technology was used to control the designed manipulator, in which the control system of the real object is replaced by a simulation model of the controller. The control of the designed manipulator is carried out in a real-time system by means of a fuzzy-logic controller. The xPC Target real-time system of the Matlab/Simulink package, and the Speedgoat Education real-time Target Machine hardware were used. The system can tune and change the parameters of the designed compensation and measurement system directly from the Simulink software in real-time during its operation. The developed models of the manipulator's simple and inverse kinematics were used in the control systems. A diagram of the control system of a planar manipulator with a closed kinematic chain is shown in Figure 3.

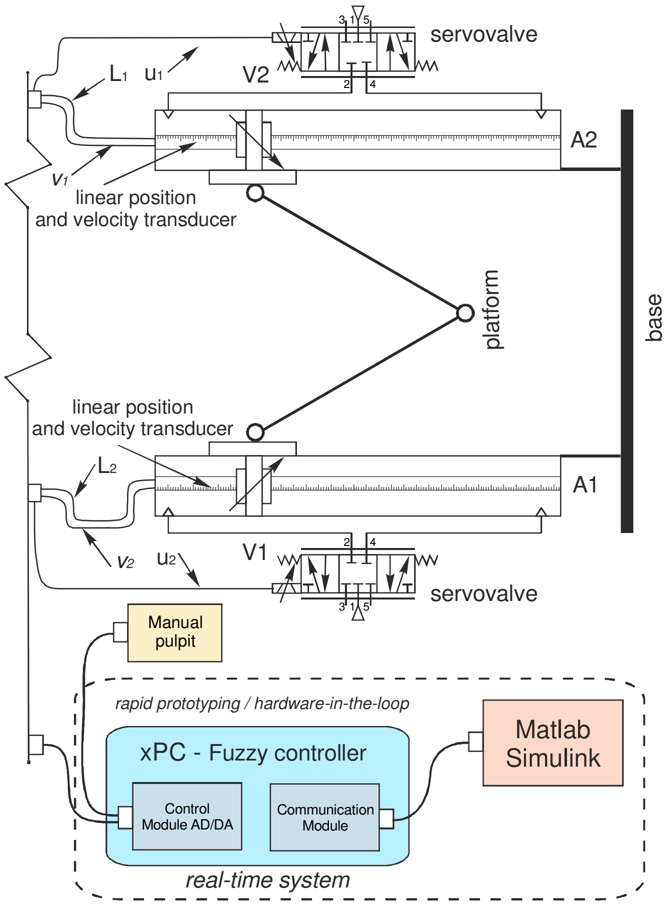

Figure 3. The diagram control system of a parallel manipulator: A1, A2—rodless actuators, V1, V2—5/3 proportional flow valves, u1, u2—voltage signals controlling the valves, L1, L2—voltage signals of the actuators' pistons, V1, V2—voltage signals of the velocity of the actuators' pistons, 1—pressure supply, 2, 4—working ports, 3, 5—exhausts.

The xPC Target real-time system of the Matlab/Simulink package is a master-slave system. Matlab/Simulink and xPC Target software were installed on the host Windows PC. The Target slave computer is the Education real-time Target Machine, which includes the real-time xPC Target and is used to execute the control program and acquire measurement data. The Host and Target computers communicate using the TCP/IP protocol. The process of designing a control system in the real-time xPC Target system of the Matlab/Simulink package requires building a block diagram in Simulink using libraries corresponding to the appropriate hardware architecture of the measurement cards used. The next stage is to compile the built control system using a compiler, e.g., C++, and then send the finished project to the Target slave computer, which starts to act as a controller. Measurement transducers and control elements were connected to the Target computer via an analog input/output card. Visualizations of the processed data and analysis of the control process are possible on the host and target computers.

4. Kinematics

In the designed structure of the manipulator, drives, in the form of pneumatic servo drives, are placed parallel to each other and at the same time constitute the basis of the manipulator. Each of the arms has only class V connections in the kinematic chain. The ends of the arms are connected with knuckle joints, creating a working platform to attach the manipulator effector. Figure 4 shows a model of a plane manipulator with two degrees of freedom with parameter designations for the kinematic model.

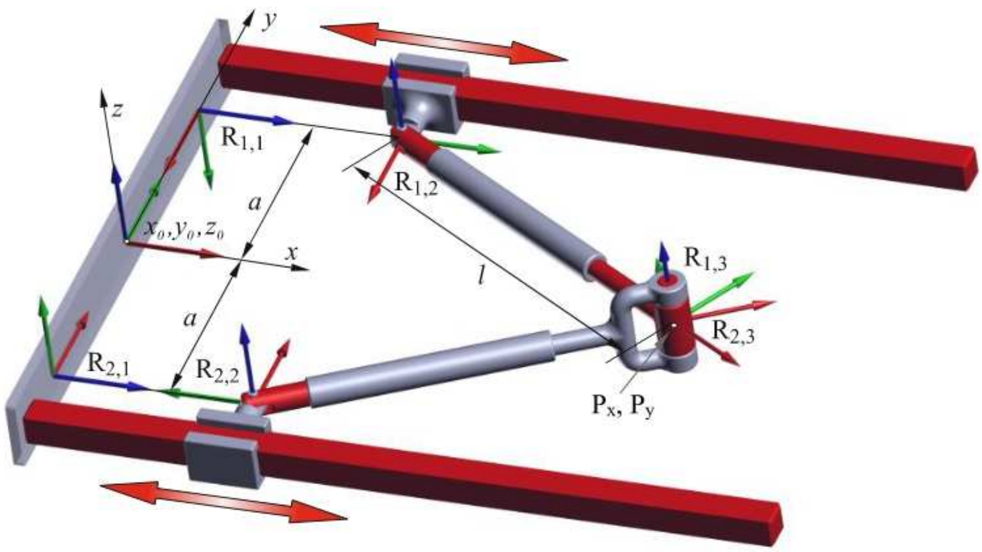

Figure 4. A model of a plane manipulator with two degrees of freedom with designations of parameters for the kinematic model (source: [8]).

Based on the parameters of the Denavit-Hartenberg (D-H) notation, the basic kinematic equations of the manipulator were determined. Tables 1 and 2 contain the kinematic parameters of the manipulator arms.

Table 1. The parameters and kinematic variables of a plane manipulator with two degrees of freedom, first arm (upper).

System Number	Θ_i	d_i	a_i	α_i
$R_{1,1}$	$-\pi/2$	0	$-a$	$-\pi/2$
$R_{1,2}$	0	$\Theta_{1.1}$	0	$\pi/2$
$R_{1,3}$	$\Theta_{1.2}$	0	l	0

Table 2. The parameters and kinematic variables of a plane manipulator with two degrees of freedom second arm (lower).

System Number	Θ_i	d_i	a_i	α_i
$R_{2,1}$	$\pi/2$	0	$-a$	$\pi/2$
$R_{2,2}$	0	$\Theta_{2.1}$	0	$-\pi/2$
$R_{2,3}$	$\Theta_{2.2}$	0	l	0

In the analyzed case, the configuration variable for the first arm is $\Theta_{1\cdot 1}$, and similarly for the second arm is $\Theta_{2\cdot 1}$. The configuration variables in the considered case of the robot do not mean rotation angles but refer to translational shifts. In the manipulator under consideration, the kinematic structure only allows the position of the effector to be discovered, without the possibility of controlling its orientation (2 degrees of freedom). The procedure assumes that a single arm of the manipulator is considered separately. As a result of subsequent rotations and translations per the D–H notation, the matrices of transformations are determined for the first and second arms. The obtained systems that define the coordinates of positions x and y should be compared to the Px and Py coordinates that define the position of the effector. Then, the solution of the system of the kinematics

Equation (1) for the first of the manipulator arms (upper) and the kinematics Equation (2) for the second of the manipulator arms (lower) is found.

$$f(\theta_{1,1}, \theta_{1,2}) = \begin{pmatrix} -P_x + \theta_{1,1} + l \sin \theta_{1,2} \\ -P_y + a - l \cos \theta_{1,2} \end{pmatrix} \tag{1}$$

$$f(\theta_{2,1}, \theta_{2,2}) = \begin{pmatrix} -P_x + \theta_{2,1} - l \sin \theta_{2,2} \\ -P_y - a + l \cos \theta_{2,2} \end{pmatrix} \tag{2}$$

5. Solving the Position of the Parallel Manipulator End Effector

Using the Delphi 6 software, a program was executed to determine the trajectory of the end effector of the manipulator. The PMS (Parallel Manipulator System) program is used to generate the coordinates of both the end effector and the corresponding slider positions. Based on the developed models of simple and inverse kinematics, the program generates a solution based on a manually specified trajectory in the main program window. Figure 5 shows the program window.

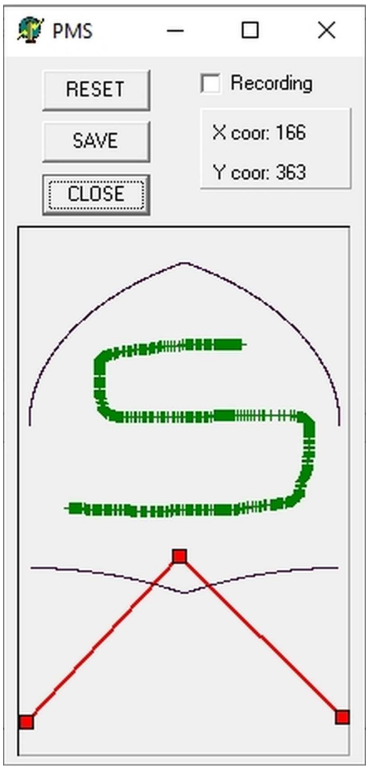

Figure 5. The main window of the PMS program.

The PMS program starts generating trajectories when the left mouse button is pressed in the end-effector action field. PMS records the positions of the end-effector and calculates the coordinates of the valve spools.

The program is built around the following elements:

- 3 buttons (save, clear window, and exit),
- chart (containing 6 data series),
- panel with two *label* text fields (showing the coordinates of the end-effector),
- a *checkbox* element (allowing to see whether the program is in save mode),
- a dialog box (for saving data).

The application allows the creation of a trajectory, which is then saved as the coordinates of the points in a text file. Using the Import Data command in Matlab software, the file can be inserted into a Matlab/Simulink model and the trajectory can then be reconstructed from the saved text file. This solution allows for the rapid planning of the end-effector trajectory at the stage of simulation studies and facilitates the introduction of changes in the positioning of the end-effector.

6. Experimental Studies

Several experimental studies were carried out on the made prototype of the planar parallel manipulator with pneumatic drive, in the same way as the simulation studies. An end-effector trajectory along the y-axis in a repetitive cycle (back and forth movement) along a section of the square-shaped trajectory and a section of the bow-shaped trajectory was examined. The graphs indicate the reference signal, output signal, and position error. Figure 6 shows the movement of the end effector along the y-axis and the displacement of the manipulator actuators.

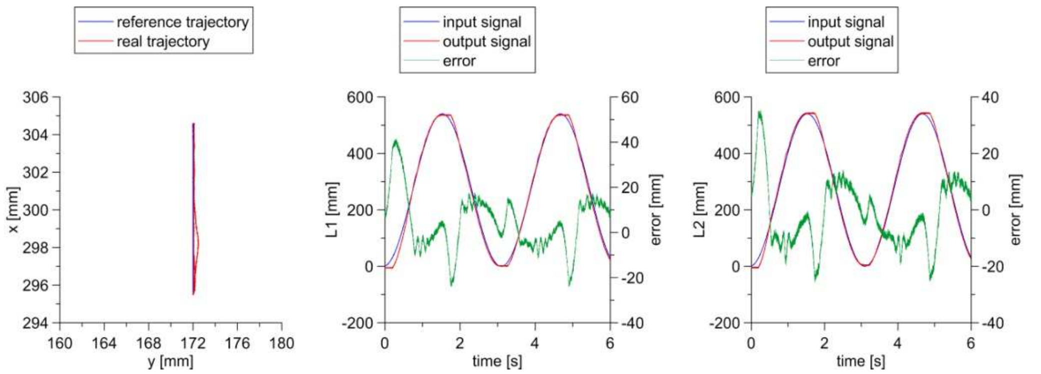

(**a**) (**b**) (**c**)

Figure 6. The positioning of the manipulator end effector along the y-axis: (**a**) end-effector trajectory, (**b**) displacement of the A1 actuator, (**c**) displacement of the A2 actuator.

Figure 7 shows the motion of the end-effector along a segment of a square–shaped trajectory and the displacements of the manipulator actuators.

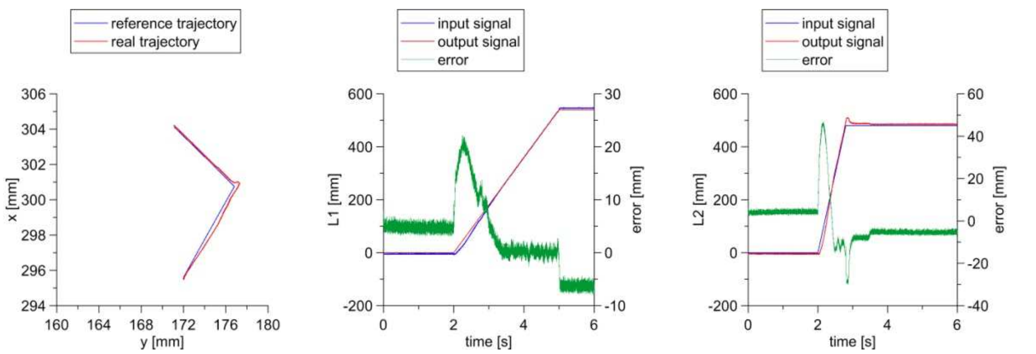

(**a**) (**b**) (**c**)

Figure 7. The positioning of the manipulator end effector along a section of the square trajectory: (**a**) end-effector trajectory, (**b**) displacement of actuator A1, (**c**) displacement of actuator A2.

Figure 8 shows the motion of the end effector along a bow-shaped trajectory and the displacement of the manipulator actuators.

Basic and integral indicators of control quality were used to assess control quality. A qualitative analysis was performed to position the end effector of the manipulator along a square trajectory for two actuators. The graphs show the control overshoot, the steady-state error within the tolerance band, the delay, the settling time, the *ISE* (Integral Square Error), and *IAE* (Integral Absolute Error) indices. The integral indices were calculated from the following equations:

$$ISE = \int_{0}^{\infty} e^2 dt \tag{3}$$

$$IAE = \int_{0}^{\infty} |e| dt \tag{4}$$

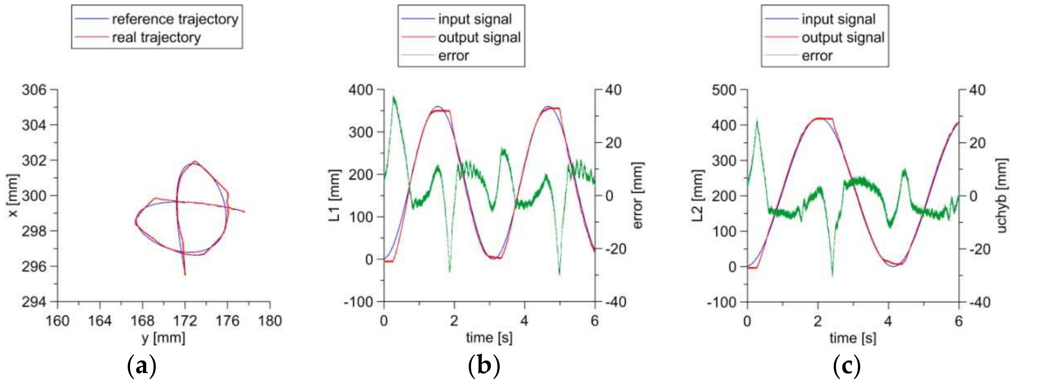

Figure 8. The positioning of the manipulator end effector along a bow-shaped trajectory: (**a**) end-effector trajectory, (**b**) displacement of actuator A1, (**c**) displacement of actuator A2.

Figure 9 shows the displacement of actuator A1, while Figure 10 shows the displacement of the actuator A2 for the motion of the end effector along a section of the square trajectory and the calculated quality indicators. The assumed steady-state error within the tolerance band 2δ was 0.28 V. For the assumed steady-state error within the tolerance band, the following results were obtained for actuator A1: overshoot σp = 0.5 V, steady-state error eust = 0.1 V and settling time tr = 4.96 s, while for the actuator A2: overshoot σp = 0.5 V, steady-state error eust = 0.1 V and settling time tr = 3.5 s.

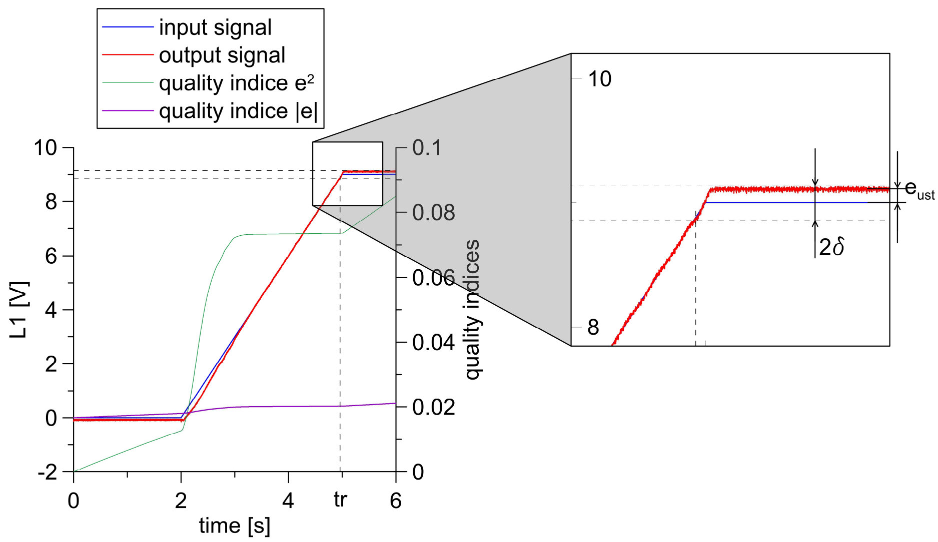

Figure 9. The dynamic characteristics and displacement analysis of actuator A1.

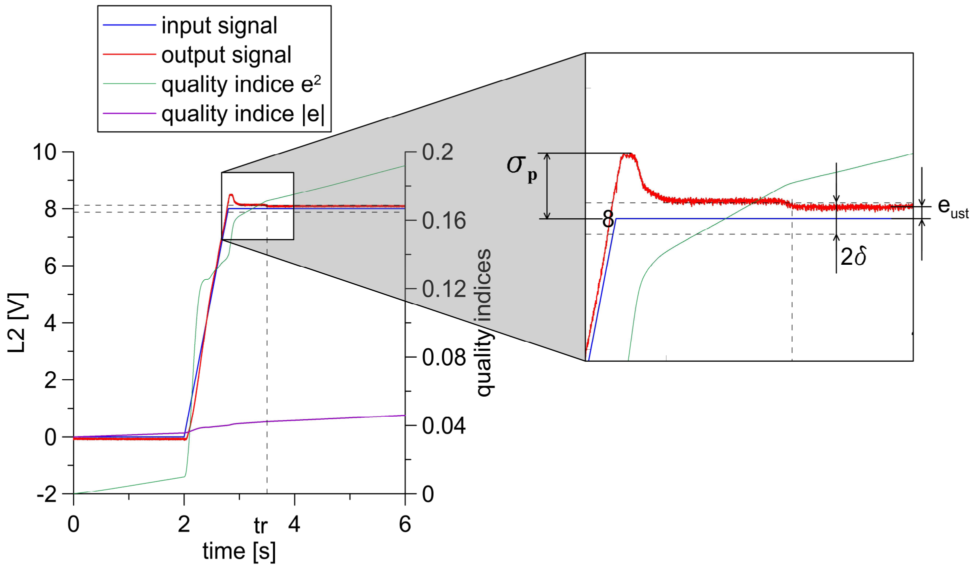

Figure 10. The dynamic characteristics and displacement analysis of actuator A2.

7. Summary and Final Conclusions

Based on the 3D model designed for a planar parallel manipulator [12], a prototype manipulator was made. A parallel manipulator control system using a PD-type fuzzy logic controller is presented. The control systems used the developed models of simple and inverse kinematics. The kinematics model designed in Matlab/Simulink was used to execute the control program.

Using Delphi 6 software, an application was developed to assist in determining the trajectory of the end effector of the manipulator. Thanks to the PMS program, planning the end-effector trajectory is easier, allowing track control in the simulation stage and verification of the correctness of the manipulator's operation.

Experimental tests were carried out on a constructed prototype of the manipulator by setting different trajectories of the end effector's movement. To analyze the quality of control, one of the preset trajectories was chosen: the motion of the end effector along a section of the squared trajectory. Basic quality indicators were calculated with an assumed steady-state error within the tolerance band of 0.28 V. For actuator A1, the settling time was 4.96 s and the determined steady-state error was 0.1 V. For actuator A2, the settling time was 3.5 s and the steady-state error was 0.1 V. The steady-state error is approximately 3%. Integral control indices such as the *ISE* integral square error and the *IAE* integral absolute error were also used.

The designed parallel manipulator can be used in industry, for example, for sorting, palletizing, or assembling parts. The application of the pneumatic drive and control system is versatile and universal. This method of control is distinguished by its cost-efficiency, positive environmental impact, and greater safety compared to other techniques. Pneumatics is recognized as one of the best methods used in manufacturing processes, but due to the compressibility of the working medium, pneumatic systems are problematic to control. The results of the experimental analysis above have shown that it is possible to develop a pneumatic control system while maintaining a high level of accuracy and repeatability in the operation of a planar manipulator.

Author Contributions: J.T.: Conceptualization, Methodology, Supervision, Project administration, Validation, Writing—review & editing; U.J.-G.: Writing—original draft, Data curation, Visualization, Validation; J.G.: Software, Visualization, Writing—review & editing. All authors have read and agreed to the published version of the manuscript.

Funding: This research received no external funding.

Data Availability Statement: Data sharing not applicable.

Conflicts of Interest: The authors declare no conflict of interest.

Abbreviations

u_1, u_2	voltage signals controlling the valves,
L_1, L_2	voltage signals of the position of the actuators' pistons,
V1, V2	voltage signals of the velocity of the actuators' pistons
P_x, P_y	coordinates of the position of the effector
ISE	Integral Square Error
IAE	Integral Absolute Error
σp	overshoot
eust	steady-state terror
tr	settling time
2δ	tolerance band

References

1. Merlet, J.P. Solving the forward kinematics of a gough-type parallel manipulator with interval analysis. *Int. J. Rob. Res.* **2004**, *23*, 221–235. [CrossRef]
2. Merlet, J.-P.; Gosselin, C.M.; Mouly, N. Workspaces of planar parallel manipulators. *Mech. Mach. Theory* **1998**, *33*, 7–20. [CrossRef]
3. Gao, F.; Liu, X.; Gruver, W.A. Performance evaluation of two-degree-of-freedom planar parallel robots. *Mech. Mach. Theory* **1998**, *33*, 661–668. [CrossRef]
4. Kang, B.; Chu, J.; Mills, J.K. Design of high speed planar parallel manipulator and multiple simultaneous specification control. In Proceedings of the 2001 ICRA IEEE International Conference on Robotics and Automation (Cat. No.01CH37164), Seoul, Republic of Korea, 21–26 May 2001; Volume 3, pp. 2723–2728. [CrossRef]
5. Gosselin, C.M.; Lemieux, S.; Merlet, J.-P. A new architecture of planar three-degree-of-freedom parallel manipulator. In Proceedings of the IEEE International Conference on Robotics and Automation, Minneapolis, MN, USA, 22–28 April 1996; Volume 4, pp. 3738–3743. [CrossRef]
6. Gao, F.; Liu, X.-J.; Chen, X. The relationships between the shapes of the workspaces and the link lengths of 3-DOF symmetrical planar parallel manipulators. *Mech. Mach. Theory* **2001**, *36*, 205–220. [CrossRef]
7. Heerah, I.; Benhabib, B.; Kang, B.; Mills, J.K. Architecture Selection and Singularity Analysis of a Three-Degree-of-Freedom Planar Parallel Manipulator. *J. Intell. Robot. Syst.* **2003**, *37*, 355–374. [CrossRef]
8. Łaski, P. *Analiza Kinematyczna Robotów Równoległych*; Wydawnictwo Politechniki Świętokrzyskiej: Kielce, Poland, 2019.
9. Ling, M.; He, X.; Wu, M.; Cao, L. Dynamic Design of a Novel High-Speed Piezoelectric Flow Control Valve Based on Compliant Mechanism. *IEEE/ASME Trans. Mechatron.* **2022**, *27*, 4942–4950. [CrossRef]
10. Bourbonnais, F.; Bigras, P.; Bonev, I.A. Minimum-Time Trajectory Planning and Control of a Pick-and-Place Five-Bar Parallel Robot. *IEEE/ASME Trans. Mechatron.* **2015**, *20*, 740–749. [CrossRef]
11. Brahmia, A.; Kelaiaia, R.; Company, O.; Chemori, A. Kinematic sensitivity analysis of manipulators using a novel dimensionless index. *Rob. Auton. Syst.* **2022**, *150*, 104021. [CrossRef]
12. Takosoglu, J.; Janus-Galkiewicz, U.; Galkiewicz, J. A Design of a 2-DoF Planar Parallel Manipulator with an Electro-Pneumatic Servo-Drive. *Energies* **2022**, *15*, 8482. [CrossRef]